University of Groningen

Quantitative three-dimensional echocardiographic analysis of the bicuspid aortic valve and aortic root

Levack, Melissa M.; Mecozzi, Gianclaudio; Jainandunsing, Jayant S.; Bouma, Wobbe; Jassar, Arminder S.; Pouch, Alison M.; Yushkevich, Paul A.; Mariani, Massimo A.; Jackson, Benjamin M.; Gorman, Joseph H.

IMPORTANT NOTE: You are advised to consult the publisher's version (publisher's PDF) if you wish to cite from it. Please check the document version below.

Document Version
Publisher's PDF, also known as Version of record

Link to publication in University of Groningen/UMCG research database

JOURNAL OF CARDIAC SURGERY WILEY

Quantitative three-dimensional echocardiographic analysis of the bicuspid aortic valve and aortic root: A single modality approach

Melissa M. Levack MD[1] | Gianclaudio Mecozzi MD[2] | Jayant S. Jainandunsing MD[3] | Wobbe Bouma MD, PhD[1,2] | Arminder S. Jassar MD[1,4] | Alison M. Pouch PhD[1] | Paul A. Yushkevich PhD[5] | Massimo A. Mariani MD, PhD[2] | Benjamin M. Jackson MD[4] | Joseph H. Gorman III MD[1,4] | Robert C. Gorman MD[1,4]

[1]Gorman Cardiovascular Research Group, University of Pennsylvania, Philadelphia, Pennsylvania

[2]Department of Cardiothoracic Surgery, University Medical Center Groningen, University of Groningen, Groningen, The Netherlands

[3]Department of Anesthesiology and Pain Medicine, University Medical Center Groningen, University of Groningen, Groningen, The Netherlands

[4]Department of Surgery, University of Pennsylvania, Philadelphia, Pennsylvania

[5]Department of Radiology, University of Pennsylvania, Philadelphia, Pennsylvania

Correspondence
Wobbe Bouma, MD PhD, Department of Cardiothoracic Surgery, University Medical Center Groningen, University of Groningen, P.O. Box 30001, Hanzeplein 1, 9700 RB Groningen, The Netherlands.
Email: w.bouma@umcg.nl

Abstract

Background: Patients with bicuspid aortic valves (BAV) are heterogeneous with regard to patterns of root remodeling and valvular dysfunction. Two-dimensional echocardiography is the standard surveillance modality for patients with aortic valve dysfunction. However, ancillary computed tomography or magnetic resonance imaging is often necessary to characterize associated patterns of aortic root pathology. Conversely, the pairing of three-dimensional (3D) echocardiography with novel quantitative modeling techniques allows for a single modality description of the entire root complex. We sought to determine 3D aortic valve and root geometry with this quantitative approach.

Methods: Transesophageal real-time 3D echocardiography was performed in five patients with tricuspid aortic valves (TAV) and in five patients with BAV. No patient had evidence of valvular dysfunction or aortic root pathology. A customized image analysis protocol was used to assess 3D aortic annular, valvular, and root geometry.

Results: Annular, sinus and sinotubular junction diameters and areas were similar in both groups. Coaptation length and area were higher in the TAV group (7.25 ± 0.98 mm and 298 ± 118 mm^2, respectively) compared to the BAV group (5.67 ± 1.33 mm and 177 ± 43 mm^2; $P = .07$ and $P = .01$). Cusp surface area to annular area, coaptation height, and the sub- and supravalvular tenting indices did not differ significantly between groups.

Conclusions: Single modality 3D echocardiography-based modeling allows for a quantitative description of the aortic valve and root geometry. This technique together with novel indices will improve our understanding of normal and pathologic geometry in the BAV population and may help to identify geometric predictors of adverse remodeling and guide tailored surgical therapy.

KEYWORDS
3D modeling, aortic valve, echocardiography

 | 1

1 | INTRODUCTION

Bicuspid aortic valve (BAV) is the most common congenital cardiac anomaly occurring in approximately 0.5% to 2.0% of live births.[1-3] This anomaly is of significant clinical relevance, given the observation that patients with BAV develop valvular dysfunction and/or proximal aortic dilatation with greater frequency than propensity-matched patients with tricuspid valves.[4-11]

Although BAV has traditionally been approached as a single clinical entity, there is significant heterogeneity with regard to patterns of valvular dysfunction. Patients may develop calcific aortic stenosis or primarily experience isolated aortic insufficiency due to a combination of cusp prolapse and/or aortic annular dilatation. Proximal aortic dilatation is also a common derivative pathology in the BAV population. This clinical heterogeneity likely reflects an underlying geometric heterogeneity in this population.[12] Sievers type 1 BAV (one raphe) is far more common than type 0 (no raphe).

Conventional two-dimensional (2D) transthoracic echocardiography (TTE) is the principal imaging technique used to identify, characterize and survey BAV. However, 2D TTE has a sensitivity of only 56% with regard to identifying BAV and is of limited utility in the characterization of morphologic subgroups and concomitant proximal aortic pathology.[13,14] While the addition of gated computed tomography (CT) and/or magnetic resonance imaging (MRI) allows for a standardized characterization of aortic geometry, not all patients are candidates for these more involved imaging techniques.[15]

Over the last decade, the introduction of real-time three-dimensional echocardiography (RT-3DE) and its recent pairing with innovative postprocessing algorithms and quantitative modeling techniques developed by our research group have allowed for the high-order characterization of 3D mitral valve geometry.[16-20] The application of modified quantitative techniques to the characterization of the aortic valve and root, as we report in the current manuscript, is a natural extension of this study (Figure 1).

We hypothesize that RT-3DE and 3D modeling can resolve subtle geometric differences in patients with BAV and TAV—for purposes of the current study, only patients with right-left cusp fusion were considered. Furthermore, we report several novel 3D measurements and indices which may ultimately aid in both the comprehensive characterization of BAV and in the development of tailored therapies for this patient population.

2 | METHODS

This study was approved by the Institutional Review Board of the University of Pennsylvania. Written informed consent was obtained from all patients.
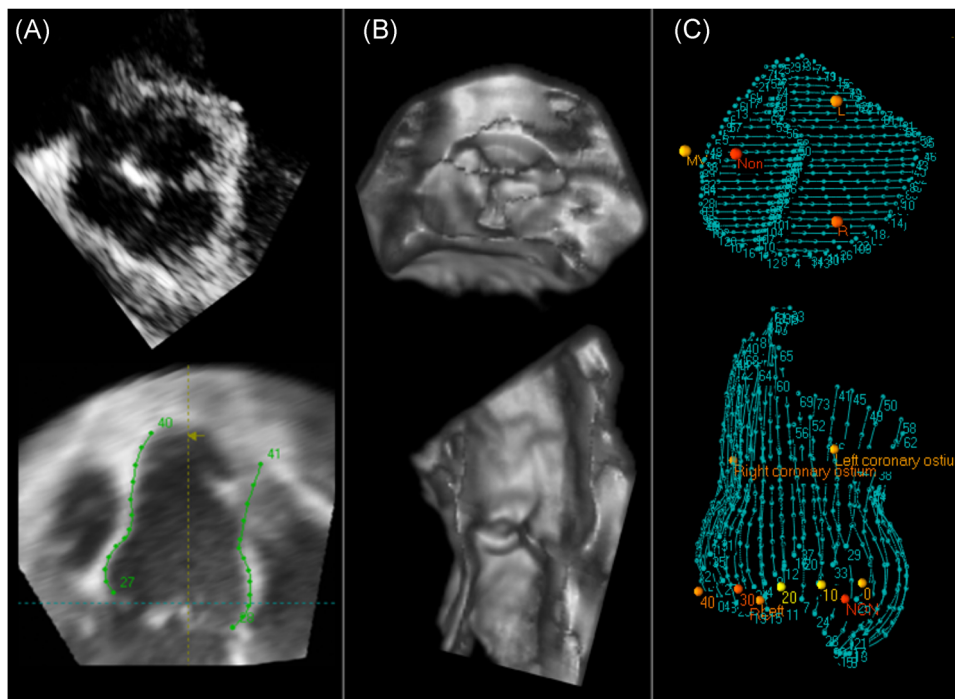
FIGURE 1 Comparison of aortic valve and root imaging techniques. A, Two-dimensional echocardiography short-axis view of the aortic valve cusps (top) and long-axis view of the aortic root (bottom). B, Raw three-dimensional echocardiography short (top) and long-axis views (bottom) of the aortic valve and root before image processing demonstrating the limited quantitative utility of 3D images alone. C, Three-dimensional reconstructed datasets demonstrating high resolution modeling of a bicuspid aortic valve and aortic root in the short (top) and long-axis views (bottom). L, left (coronary cusp); MV, mitral valve; Non, noncoronary cusp; R, right (coronary cusp)

2.1 | Patients and image acquisition

Three-dimensional transesophageal echocardiograms were acquired for 10 patients (5 patients with TAV and 5 patients with a BAV with right-left cusp fusion) with normal ejection fraction, a root diameter less than 4.2 cm, and no evidence of valvular dysfunction. All patients underwent transesophageal echocardiography (TEE) for diagnostic purposes unrelated to aortic root pathology. TEE examinations were performed under light sedation by an experienced cardiologist in the echocardiography laboratory at the Hospital of the University of Pennsylvania. Electrocardiographically-gated, full-volume datasets were acquired using an iE-33 platform (Philips Medical Systems, Andover, MA) equipped with a 2 to 7 MHz X7-2t TEE matrix-array transducer. Care was taken to acquire the entire aortic root complex in each case.

2.2 | Image segmentation

Each full-volume 3D dataset was exported to an Echo-View 5.4 (TomTec Imaging Systems, Munich, Germany) software workstation for image analysis. This customized software allowed for interactive manipulation including rotation, translation, surface rendering, and measurement of full 3D datasets. All analyses were performed at the end-diastole.

The plane of the aortic valve orifice was rotated into a short-axis view. The geometric center of the aortic valve was then translated to the intersection of two orthogonal long-axis planes of the aortic root. A rotational template consisting of 18 long-axis cross-sectional planes separated by 10° increments was superimposed on the 3D image (Figure 2). Annular points were identified on each of the 18 long-axis rotational planes. Freehand curves were constructed from the annular points along the height of the root at each rotational

plane for root reconstruction. The sinotubular junction (STJ) was manually identified in each plane.

The cusps were segmented in parallel long-axis cross-sections spaced 1 mm apart (Figure 3). TAV cusps were segmented in pairs along each of the three coaptation zones (ie, right-left, left-non, and right-non zones). BAV cusps were segmented along the functional intercommissural line between the fused and the unfused cusps. The coaptation zones between all cusps were independently identified in each parallel cross-section. Datasets, each comprising 600 to 1200 individual data points, were created for each valve. The Cartesian coordinates of the segmented annulus, root, cusps, and coaptation zones were exported to Matlab (The Mathworks Inc, Natick, MA) for image postprocessing and quantitative analysis by means of a series of well-characterized custom algorithms.

2.3 | Annular and root analysis

The datasets were translated to the origin based on the center of gravity of their respective point clouds. The least-squares plane of the data point cloud for the STJ was aligned to the x-y plane. The plane defined by the lowest point in each of the three sinus segments was designated the basal annular plane. The plane parallel to the annular plane and encompassing the maximum area of the root was defined as the sinus plane. Annular area, sinus area, and STJ area were calculated as were their interdependent ratios.

Novel indices of valvular and root geometry were derived to allow for a comprehensive, quantitative description of the aortic root complex. Coaptation height was defined as the mean vertical displacement of the intercommisural lines above the basal annular plane. The subvalvular tenting index was defined as the fractional aortic root volume subtended by the valvular surface, divided by the cross-sectional area of the aortic valve annulus. The supravalvular tenting index was defined as the
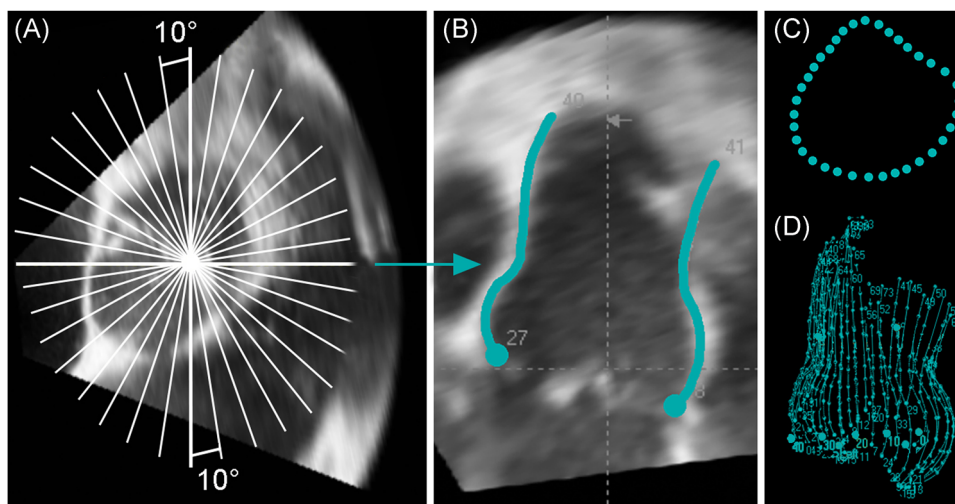
FIGURE 2 Annular and root segmentation technique. A, Short-axis view containing the (bicuspid) aortic valve with cross-sectional planes at 10-degree increments (resulting in a total of 18 cross-sectional planes and 36 annular data points). B, Long-axis view through a cross-sectional plane with annular points (blue dots) and the root tracings (blue lines). C, Annular view of a single real-time 3D-derived aortic annular model with the 36 annular data points. D, Side view of a single real-time 3D-derived aortic root model. 3D, three-dimensional
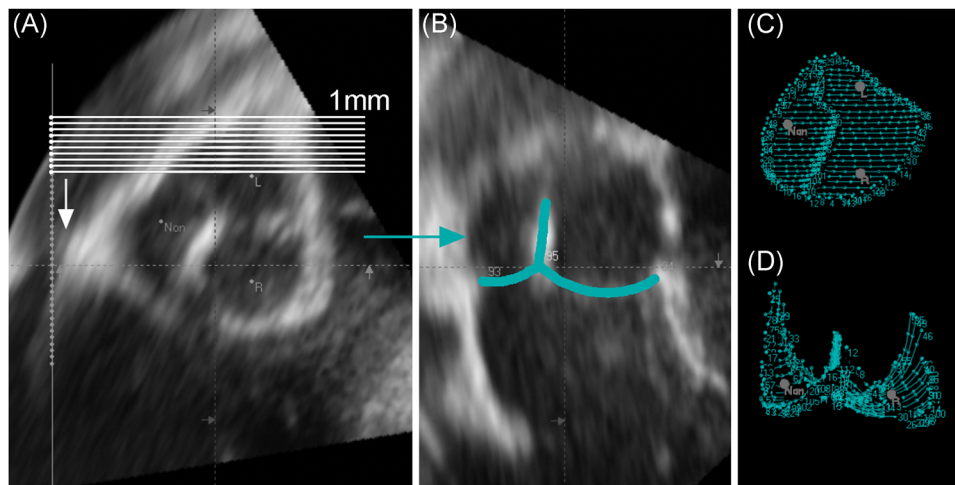
FIGURE 3 Cusp segmentation technique. A, Short-axis view containing the (bicuspid) aortic valve and parallel transverse cross-sections every 1 mm along the functional intercommissural line between fused and unfused cusps. B, One of the 2D cross-sections; the surface of the aortic cusps and the coaptation zone is interactively traced (blue lines). C, Annular view of the completed 3D cusp segmentation model. D, Side view of the completed 3D cusp segmentation model. L, left (coronary cusp); Non, noncoronary cusp; R, right (coronary cusp); 3D, three-dimensional; 2D, two-dimensional

fractional aortic root volume above the valvular surface, divided by the cross-sectional area of the aortic valve annulus.

2.4 | Cusp and coaptation analysis

Smoothing splines were constructed for each cusp using the Matlab "thin-plate smoothing spline" function, with the variable smoothing parameter assigned by the software. The resulting surface splines were meshed for 3D surface rendering. Individual cusp and coaptation areas were determined for each valve as was the average coaptation length along each of the intercommissural lines.

2.5 | Statistical analysis

Continuous variables were expressed as mean ± standard deviation. Categorical variables were expressed as percentages. Comparisons between groups were performed using Pearson's χ^2 test or Fisher's exact test (two-sided) as appropriate for categorical variables and the independent samples t test or the Mann-Whitney U test (two-sided) as appropriate for continuous variables.

All calculations were performed using SPSS Statistics (IBM SPSS Statistics 22.0; IBM Corporation, Chicago, IL). Statistically significant differences were established at $P < .05$.

3 | RESULTS

3.1 | Baseline patient characteristics

Patient characteristics are presented in Table 1. Patients in the BAV group were younger than patients in the TAV group, $P = .01$. There were

no differences in 2D annular, sinus, or STJ diameter measurements between groups as measured with standard 2D echocardiography. All patients were similar in terms of left ventricular ejection fraction.

3.2 | Aortic root cross-sectional areas

2D projected annular area, sinus area, and STJ area as determined by means of 3DE image analysis are shown in Table 2. Ratios describing the relationship between each of the cross-sectional planes (annulus: sinus: STJ) were calculated for both groups. For the TAV group the ratio was 1:1.84:1.25 and for the BAV group it was 1:1.35:1.10 (Figure 4).

3.3 | Cusp surface areas

Surface areas for the left, noncoronary, and right TAV cusps were 194 ± 29, 174 ± 32, and 188 ± 46 mm^2, respectively. The unfused

TABLE 1 Baseline patient characteristics

Variable/parameter[a]	TAV (n = 5)	BAV (n = 5)	P value
Age, y	64.8 ±10.7	28.3 ± 20.6	.01
Female	3 (60)	1 (20)	.52
LVEF, %	61.0 ± 6.5	60.0 ± 3.5	.77
Aortic valve annular diameter, cm	2.54 ± 0.38	3.04 ±0.61	.61
Sinus diameter, cm	3.38 ±0.4	3.50 ±0.64	.73
Sinotubular junction diameter, cm	2.92 ±0.22	2.90 ± 0.60	.95

Abbreviations: BAV, bicuspid aortic valve; LVEF, left ventricular ejection fraction; TAV, tricuspid aortic valve.
[a]Data were presented as mean±standard deviation or number (%).

TABLE 2 Three-dimensional aortic annular, valvular, and root geometry

Parameter[a]	TAV (n = 5)	BAV (n = 5)	P value
Aortic root cross-sectional areas			
Annular area, mm^2	428 ±47	622 ± 239	.11
Sinus area, mm^2	787 ±78	845 ± 318	.70
Sinotubular junction area, mm^2	533 ± 25	682 ± 289	.28
Cusp surface areas			
Cusp surface area: annular area ratio	1.26 ± 0.03	1.25 ±0.05	.65
Coaptation zones			
Coaptation length, mm	7.25 ±0.98	5.67 ±1.33	.07
Coaptation area, mm^2	298 ± 118	177 ± 43	.01
Cusp tenting and remodeling indices			
Coaptation height, mm	4.80 ± 0.62	5.13 ± 0.87	.91
Subvalvular tenting index	2.73 ±0.58	2.49 ±0.49	.65
(Index of cusp flattening)			
Supravalvular tenting index	18.39 ± 2.55	20.97 ± 3.84	.57
(Index of root remodeling)			

Abbreviations: BAV, bicuspid aortic valve; TAV, tricuspid aortic valve.
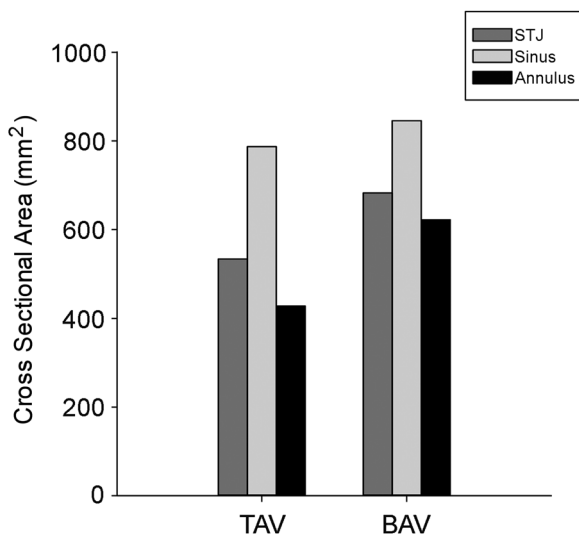[a]Data were presented as mean±standard deviation.

FIGURE 4 Comparison of TAV and BAV cross-sectional aortic areas. In the TAV group, there is a preserved relationship between the three cross-sectional areas: the annular: STJ ratio approximates 1:1 in normally functioning valves and there is a distinct size difference between the sinus area and STJ area. In the BAV group, even though these were all normally functioning valves, there is relative effacement of the STJ as the difference between the sinus area and STJ areas are less. Moreover, in the BAV group there is a trend towards annular and STJ dilatation. BAV(s), bicuspid aortic valve(s); STJ, sinotubular junction; TAV(s), tricuspid aortic valve(s)

noncoronary cusp in the BAV group was 312 ± 100 mm^2 (P = .02, vs noncoronary TAV cusp). The total fused cusp surface area was 469 ± 207 mm^2 for the BAV group compared to 382 ± 41 mm^2 for the total area of the corresponding right and left coronary cusps in the TAV group (P = .39). A representative three-dimensional rendering of these areas is shown in Figure 5. The cusp surface area to annular area ratios was similar in both groups.

3.4 | Coaptation zones

Mean coaptation length and coaptation area for the TAV and BAV groups are shown in Table 2. Coaptation area was significantly higher in the TAV group compared to the BAV group. A representative three-dimensional rendering of the coaptation areas is shown in Figure 5.

3.5 | Cusp tenting and remodeling indices

Cusp tenting and remodeling indices are shown in Table 2. These indices were similar among TAV and BAV groups.

4 | DISCUSSION

Aortic valve replacement has long been the gold standard for aortic valve pathology. However, both aortic valve-sparing root procedures and primary valve repair procedures have increased in popularity over the past two decades and have become the de facto standard of care for certain patterns of root and/or isolated valve pathology.[21] As a consequence, there is a significant clinical need for both a coherent geometric lexicon and a standardized approach to surgical planning and postoperative surveillance. To date, the determination of valve repairability is based on a series of 2D measurements, intraoperative assessment, and surgical intuition. As a consequence, the majority of valve repair operations are performed at high-volume centers with considerable institutional expertise in aortic surgery. As excellent outcomes have been reported for nearly all patterns of root pathology, valve-repair procedures, including those for BAV patients, are increasingly regarded as the standard of care at certain levels of institutional acuity.[22-24]

Echocardiographically derived, interactive 3D models of the aortic root complex allow for a detailed, quantitative description of root geometry. In the current study, we compare relevant features of TAV and BAV root geometry and propose several potentially useful indices that cannot be derived by means of conventional imaging techniques. These novel indices may ultimately provide rational geometric targets in patients undergoing valve-sparing operations and may provide a more quantitative and reproducible means of characterizing root complex geometry in high-risk patients undergoing surveillance. Our data confirms previous observations that the bicuspid root complex is geometrically distinct from the tricuspid
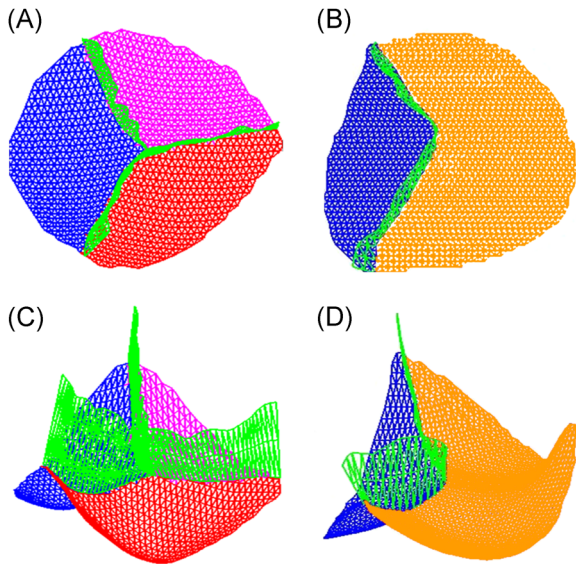
FIGURE 5 Three-dimensional mesh rendering of a representative tricuspid (A,C) and bicuspid aortic valve (B,D). Both top-down (A,B) and side views (C,D) are shown for comparison. The TAV noncoronary cusp (depicted in blue) is notably smaller when compared to the corresponding BAV noncoronary/unfused cusp (also depicted in blue). Additionally, the BAV valve demonstrates significantly less cusp coaptation overall (depicted in green). Color coding: blue, noncoronary cusp; Red, right coronary cusp; purple, left coronary cusp; orange, left-right fused cusp; green, cusp coaptation. BAV, bicuspid aortic valve; TAV, tricuspid aortic valve

root complex.[25,26] In both of our study cohorts the STJ to annular ratio was preserved, (TAV=1.24; BAV=1.09), confirming that adverse root remodeling had not occurred in either cohort, although the BAV cohort patients are younger. However, the mid-sinus to annular ratio was significantly lower in the BAV cohort (1.35 vs 1.8; $P = .03$) while the STJ to mid-sinus ratio was higher (0.87 vs 0.67), suggesting that there is relative effacement of the root in BAV compared to TAV roots. In other words, the sinus segment is less pronounced (less "curvy") in BAV roots. This would tend to increase wall stress in both the sinus segment and the supra-sinus proximal ascending aorta and may contribute to the propensity of these two regions to undergo adverse remodeling in this patient population. Broader application of the quantitative modeling techniques described herein will ultimately improve our understanding of BAV and its derivative pathologies. Furthermore, these techniques have the potential to identify high-risk geometric features in patients that will benefit from early intervention to prevent adverse root remodeling.

Interestingly, marked differences were noted with regard to the distribution of cusp surface area in the BAV and TAV cohorts. This is particularly relevant in the BAV cohort as our data confirms the long-held understanding that both the size and radial distribution of the fused cusp lies somewhere between 50/50 and 66/33. Given the well-documented need to maintain or reproduce native patterns of cusp symmetry during aortic valve repair and/or valve-sparing root replacement,[27] a thorough understanding of these patterns of 3D asymmetry is essential to optimizing repair efficacy and durability. It

is also worth noting that while the cusp surface area to annular area ratios was similar between the two cohorts, coaptation areas were not ($P = .01$). This relative paucity of cusp coaptation surface in the BAV cohort may contribute to the propensity of these valves to undergo structural and functional deterioration.

Although 2D interrogation of the aortic root complex (customarily obtained using echocardiography) has proven an effective means for quantifying aortic root dilatation, accurate assessment of cusp morphology, and geometry remains challenging. All structural components of the aortic root complex are geometrically and functionally interrelated and cannot be characterized in isolation, nor can they be accurately characterized in 2D space as each component is a fully 3D structure. The relevance of 3D geometry with regard to valve repair has been previously addressed by several leaders in the field of aortic surgery.[28] The term "effective height," defined as the vertical displacement of the free edge margins above the basal annular plane, was first described in literature by Schäfers et al[28] and is commonly examined as an intraoperative index of native cusp prolapse both before and after cusp and/or root repair and thus allows for the quantitative assessment of disease severity and repair adequacy.

Echocardiographically derived 3D aortic root modeling, as described in the current study (coaptation height), facilitates the description of the same parameter and allows for the integration of this parameter into the preoperative characterization of the valve and/or root repairability. Furthermore, longitudinal assessment of 3D aortic root geometry has great potential with regard to elucidating patterns of function and failure in patients who have undergone valve-sparing operations. Multiple 2D echocardiographic predictors of early repair failure have been proposed by several experienced surgeons. Nearly all of these proposed indexes attempt to quantify the adequacy of commissural elevation and cusp coaptation following repair.[29,30] However, it has been repeatedly shown that 2D measurements of geometrically complex intracardiac structures are highly dependent on plane selection and operator experience, thus significantly limiting the quantitative and predictive power of the proposed indexes.[31,32] The indexes proposed in the current study are either fully 3D or are directly derived from an interactive 3D model. As an example, we describe the sub- and supra-valvar tenting index, which (when paired) provide a means of describing the adequacy of both commissural elevation and cusp coaptation for the entire aortic root complex. Similarly, the cusp coaptation area provides a coherent description of coaptation behavior for the entire root as opposed to that occurring at a single, selected long-axis plane. The series of 3D or 3D-derived indexes described in the current study has significant potential to aid in both the preoperative assessment of valve repairability and postoperative surveillance of repair durability. Data acquired therein may ultimately provide a geometrically rational means of constructing patient-specific, tailored, repair (or replacement) strategies.

Previous work from our group has shown a correlation between measurements derived from conventional 2D echo assessment and 3D modeling for TAV.[33] Intermodality agreement for 2D and 3D

techniques was again observed in the current study for both cohorts, though this was not considered a rational means of measurement validation and was not included in the data summary. It is our opinion that additional and more rigorous validation of these modeling techniques involving both documentation of intraoperator reproducibility and assessment of intermodality agreement (gated CT, cardiac MRI) is necessary before making any rigorous conclusions. Another limitation of this study, particularly with regard to the BAV cohort, is that "normal" is a time-dependent moving data point and is difficult to define with respect to study inclusion criteria as patterns of remodeling in this population are unpredictable and often subtle. To date, most clinicians advocate routine monitoring of these patients to evaluate functional changes of the cusps, ejection fraction, remodeling of the left ventricle and remodeling of the root, thus defining "normal" in the context of the individual patient. Finally, it was not possible to match subjects for age in the current study. In fact, the BAV cohort was significantly younger than the corresponding TAV cohort.

In conclusion, while the clinical utility of 2D echocardiography and gated CT imaging is indisputable, the current study demonstrates that 3D echocardiography may represent an important adjunctive technology with regard to both preoperative characterization of patterns of root pathology and postoperative surveillance. This is particularly true in BAV populations, where 3D root asymmetry is well-documented and traditional 2D characterizations can be of limited utility.

CONFLICT OF INTERESTS

The authors declare that there are no conflict of interests.

ORCID

Wobbe Bouma http://orcid.org/0000-0003-3271-8220

REFERENCES

1. Nistri S, Basso C, Marzari C, Mormino P, Thiene G. Frequency of bicuspid aortic valve in young male conscripts by echocardiogram. *Am J Cardiol.* 2005;96:718-721.
2. Tutar E, Ekici F, Atalay S, Nacar N. The prevalence of bicuspid aortic valve in newborns by echocardiographic screening. *Am Heart J.* 2005; 150:513-515.
3. Basso C, Boschello M, Perrone C, et al. An echocardiographic survey of primary school children for bicuspid aortic valve. *Am J Cardiol.* 2004;93:661-663.
4. Beroukhim RS, Kruzick TL, Taylor AL, Gao D, Yetman AT. Progression of aortic dilation in children with a functionally normal bicuspid aortic valve. *Am J Cardiol.* 2006;98:828-830.
5. Warren AE, Boyd ML, O'Connell C, Dodds L. Dilatation of the ascending aorta in paediatric patients with bicuspid aortic valve: frequency, rate of progression and risk factors. *Heart.* 2006;92: 1496-1500.
6. Holmes KW, Lehmann CU, Dalal D, et al. Progressive dilation of the ascending aorta in children with isolated bicuspid aortic valve. *Am J Cardiol.* 2007;99:978-983.
7. La Canna G, Ficarra E, Tsagalau E, et al. Progression rate of ascending aortic dilation in patients with normally functioning bicuspid and tricuspid aortic valves. *Am J Cardiol.* 2006;98:249-253.
8. Davies RR, Kaple RK, Mandapati D, et al. Natural history of ascending aortic aneurysms in the setting of an unreplaced bicuspid aortic valve. *Ann Thorac Surg.* 2007;83:1338-1344.
9. Yasuda H, Nakatani S, Stugaard M, et al. Failure to prevent progressive dilation of ascending aorta by aortic valve replacement in patients with bicuspid aortic valve: comparison with tricuspid aortic valve. *Circulation.* 2003;108:291-294.
10. Ward C. Clinical significance of the bicuspid aortic valve. *Heart.* 2000; 83:81-85.
11. Chan KL, Ghani M, Woodend K, Burwash IG. Case-controlled study to assess risk factors for aortic stenosis in congenitally bicuspid aortic valve. *Am J Cardiol.* 2001;88:690-693.
12. Fedak PW. Bicuspid aortic valve syndrome: heterogeneous but predictable? *Eur Heart J.* 2008;29:432-433.
13. Otani K, Takeuchi M, Kaku K, et al. Assessment of the aortic root using real-time 3D transesophageal echocardiography. *Circ J.* 2010; 74:2649-2657.
14. Alegret JM, Palazón O, Duran I, Vernis JM. Aortic valve morphology definition with transthoracic combined with transesophageal echocardiography in a population with high prevalence of bicuspid aortic valve. *Int J Cardiovasc Imaging.* 2005;21:213-217.
15. Buchner S, Hulsmann M, Poschenrieder F, et al. Variable phenotypes of bicuspid aortic valve disease: classification by cardiovascular magnetic resonance. *Heart.* 2010;96:1233-1240.
16. Ryan LP, Salgo IS, Gorman RC, Gorman JH. The emerging role of three-dimensional echocardiography in mitral valve repair. *Semin Thorac Cardiovasc Surg.* 2006;18:126-134.
17. Ryan LP, Jackson BM, Enomoto Y, et al. Description of regional mitral annular nonplanarity in healthy human subjects: a novel methodology. *J Thorac Cardiovasc Surg.* 2007;134:644-648.
18. Ballocca F, Meier LM, Ladha K, Qua Hiansen J, Horlick EM, Meineri M. Validation of quantitative 3-dimensional transesophageal echocardiography mitral valve analysis using stereoscopic display. *J Cardiothorac Vasc Anesth.* 2019;33:732-741.
19. Noack T, Kiefer P, Ionasec R, et al. New concepts for mitral valve imaging. *Ann Cardiothorac Surg.* 2013;2:787-795.
20. Jolley MA, Ghelani SJ, Adar A, Harrild DM. Three-dimensional mitral valve morphology and age-related trends in children and young adults with structurally normal hearts using transthoracic echocardiography. *J American Soc of Echocardiography.* 2017;30: 561-571.
21. Ho SY. Structure and anatomy of the aortic root. *Eur J Echocardiogr.* 2009;10:3-10.
22. David TE. Aortic valve sparing operations. *Semin Thorac Cardiovasc Surg.* 2011;23:146-148.
23. Leshnower BG, Guyton RA, Myung RJ, et al. Expanding the indications for the David V aortic root replacement: early results. *J Thorac Cardiovasc Surg.* 2012;143:879-884.

24. Boodhwani M, de Kerchove L, Glineur D, et al. Repair of regurgitant bicuspid aortic valves: a systematic approach. *J Thorac Cardiovasc Surg*. 2010;140:276-284.

25. Conti CA, Della Corte A, Votta E, et al. Biomechanical implications of the congenital bicuspid aortic valve: a finite element study of aortic root function from in vivo data. *J Thorac Cardiovasc Surg*. 2010;140:890-896.

26. Khoury GE, Glineur D, Rubay J, et al. Functional classification of aortic root/valve abnormalities and their correlation with etiologies and surgical procedures. *Curr Opin Cardiol*. 2005;20:115-121.

27. David TE. Aortic valve haemodynamics after aortic valve-sparing operations. *Eur J Cardiothorac Surg*. 2012;41:788-789.

28. Schäfers HJ, Bierbach B, Aicher D. A new approach to the assessment of aortic cusp geometry. *J Thorac Cardiovasc Surg*. 2006;132:436-438.

29. Pethig K, Milz A, Hagl C, Harringer W, Haverich A. Aortic valve reimplantation in ascending aortic aneurysm: risk factors for early valve failure. *Ann Thorac Surg*. 2002;73:29-33.

30. le Polain de Waroux JB, Pouleur AC, Robert A, et al. Mechanisms of recurrent aortic regurgitation after aortic valve repair: predictive value of intraoperative transesophageal echocardiography. *JACC Cardiovasc Imaging*. 2009;2:931-939.

31. Hibberd MG, Chuang ML, Beaudin RA, et al. Accuracy of three-dimensional echocardiography with unrestricted selection of imaging planes for measurement of left ventricular volumes and ejection fraction. *Am Heart J*. 2000;140:469-475.

32. Houck RC, Cooke JE, Gill EA. Live 3D echocardiography: a replacement for traditional 2D echocardiography? *Am J Roentgenol*. 2006;187:1092-1106.

33. Jassar AS, Levack MM, Solorzano RD, et al. Feasibility of in vivo human aortic valve modeling using real-time three-dimensional echocardiography. *Ann Thorac Surg*. 2014;97:1255-1258.